Growth and optical properties of transparent $CaMoO_4$ films by chemical solution deposition on Si and glass substrates

2009 J. Phys. D: Appl. Phys. 42 045404

(http://iopscience.iop.org/0022-3727/42/4/045404)

IOP PUBLISHING JOURNAL OF PHYSICS D: APPLIED PHYSICS

J. Phys. D: Appl. Phys. **42** (2009) 045404 (6pp) doi:10.1088/0022-3727/42/4/045404

Growth and optical properties of transparent $CaMoO_4$ films by chemical solution deposition on Si and glass substrates

Hechang Lei, Xuebin Zhu, Shoubao Zhang, Gang Li, Xianwu Tang, Wenhai Song, Zhaorong Yang, Jianming Dai and Yuping Sun

Key Laboratory of Materials Physics, Institute of Solid State Physics, Chinese Academy of Sciences, Hefei 230031, People's Republic of China

E-mail: ypsun@issp.ac.cn

Received 2 September 2008, in final form 31 October 2008
Published 15 January 2009
Online at stacks.iop.org/JPhysD/42/045404

Abstract

Nanocrystalline $CaMoO_4$ (CMO) thin films were fabricated on Si and glass substrates via the chemical solution deposition (CSD) method. From x-ray diffraction , atomic force microscopy and Fourier transform infrared spectra results, relatively smooth Scheelite-type CMO thin films can be fabricated within the annealing temperature range from 400 to 700 °C. The band gap is 4.18 eV calculated from the optical transmission spectra and the photoluminescence (PL) emission spectra show that the CMO thin films on Si have a broad green emission band centred at 490 nm. Our experimental results show that the CSD method is an alternative method to prepare nanocrystalline CMO thin films with a great PL property at low annealing temperatures.

(Some figures in this article are in colour only in the electronic version)

1. Introduction

Metal molybdates of relatively large bivalent cations ($RMoO_4$, M = Ca, Ba, Sr, Pb) exist in the so-called Scheelite structure, where the molybdenum atom adopts tetrahedral coordination [1]. This kind of material has been widely studied due to its optical properties. For example, it can be used as laser host material, photoluminescence (PL) material and intrinsic scintillation material [2–4]. $CaMoO_4$ (CMO) as a kind of Scheelite-type material has excellent properties of green luminescence and a high application potential in microwave devices [5, 6].

CMO single crystal and powder have been fabricated successfully by a large number of methods such as the Czochralski technique [7], conventional solid state reactions [8] and the hydrothermal method [9]. Nevertheless, compared with single crystals and powders, the preparation of CMO thin films has been less investigated and the most common method is the electrochemical route [10, 11]. However, the electrochemical method is limited since only Mo substrates can be used to prepare CMO films. For more applications, CMO thin films should be deposited on other different substrates. On the other hand, in order to avoid the volatilization of MoO_3 during the preparation process [12], it is necessary to synthesize crystallized CMO films at medium or even low temperatures. The chemical solution deposition (CSD) method is an alternative way to prepare such films. The CSD method, as a highly versatile method to fabricate oxide thin films, combines the advantages of inexpensive non-vacuum equipment, precise control of precursor stoichiometry, ease of compositional modification, low synthesis temperature and high deposition rates in large areas. Many oxide thin films have been fabricated via this method [13–15] and $SrMoO_4$ (SMO) thin films on Si substrates using the CSD method have also been prepared by our group [16].

In this work, systematic investigations on the preparation, characterization and optical properties of crystallized CMO thin films on Si and glass substrates using the CSD method are presented, and it should be pointed out that there are no reports on the deposition of CMO on glass.

2. Experiments

The fabrication procedure of CMO thin films is similar to that of SMO thin films [16]. In short, ammonium para-molybdate (purity 99%) and citric acid monohydrate (CA, purity 99.5%) (molar ratio, Mo : CA = 1 : 1) were first dissolved in ethylene glycol (EG, purity 99.5%) (Mo : EG = 1 mol : 1.5 L) and stirred continuously under a magnetic stirrer at 30 °C for about 2 h until the solution became totally transparent; then 10 ml of acetic acid glacial (HOAc, purity 99.5%) (Mo : HOAc = 1 mol : 5 L) was added into the solution and stirred for about 20 min at 30 °C. The third step was to dissolve stoichiometric calcium acetate (purity 99%) into the mixture solution and stir for more than 4 h at room temperature. Finally, the as-prepared solution was filtered with a 0.2 μm filter to eliminate particulates from the solution. The final solution was of about 0.2M concentration.

The (1 0 0)-oriented Si wafers and soda-lime glass were used as substrates. Before depositing CMO thin films, both substrates were degreased in acetone and ethanol using an ultrasonic cleaner for 10 min, respectively. The films were spin-coated on Si and glass substrates using rotation speeds of 4500 rpm for 10 s and 6000 rpm for 10 s, respectively. The as-spun films were pyrolyzed in air at 350 °C for 20 min in a resistive furnace. The thicker films were prepared by repeating the above processes five times. Then the pyrolyzed CMO thin films were annealed at different temperatures from 400 to 900 °C for 2 h in air.

The crystallization and the micromorphology of the prepared CMO thin films were characterized using an x-ray diffractometer (XRD, Philips-designed X'Pert Pro type) and atomic force microscopy (AFM, Park Scientific Instruments designed, Autoprobe CP type). The film thickness was measured by a field emission scanning electronic microscope (FE-SEM; FEI-designed Sirion 200 type). Optical transmittance measurements were carried out within the wavelength range 200–800 nm using a UV–Vis–NIR spectrophotometer (CARY-5E) at a fixed incidence angle perpendicular to the films. Fourier transform infrared spectroscopy (FT-IR) transmission spectra for CMO thin films on Si were recorded in the frequency range 400–2000 cm^{-1} using a Nicolet Magna 750 operating in transmission mode. The PL measurement was carried out using a pulsed Ti: sapphire laser at an excitation wavelength of 266 nm and the maximum output power of the laser was 20 mW. All measurements were taken at room temperature.

3. Results and discussion

Figure 1(a) gives the XRD patterns of the CMO thin films pyrolyzed at 350 °C for 20 min. It is shown that the CMO thin film pyrolyzed at 350 °C is still amorphous. The CMO film annealed at 400 °C for 2 h starts to display the Scheelite type phases (figure 1(b), JCPDS No 07-0212). Furthermore, from figures 1(c)–(g), it can be concluded that the crystallization of the CMO films is improved with the increase in the annealing temperature. When the annealing temperature is increased to 900 °C, the (1 0 1) diffraction peak of SiO_2 (quartz type) appears, which suggests that the Si substrates are oxidized to some extent at high annealing temperatures.

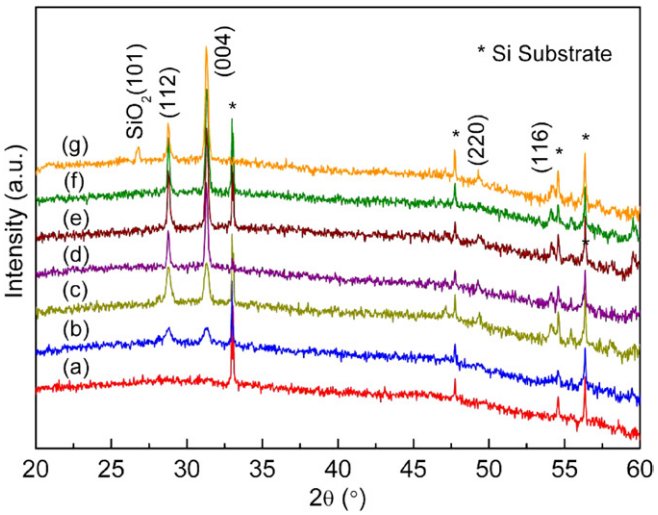

Figure 1. XRD patterns of CMO thin films pyrolyzed at 350 °C for 20 min (a) and annealed at 400 °C (b), 500 °C (c), 600 °C (d), 700 °C (e), 800 °C (f), 900 °C (g) for 2 h on Si substrates.

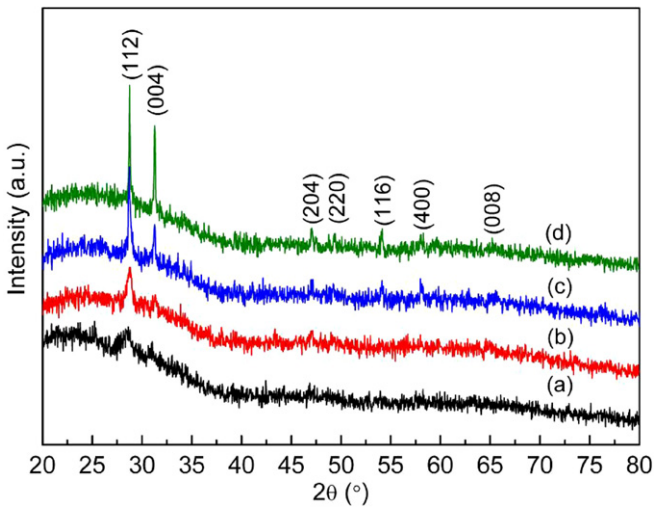

Figure 2. XRD patterns of CMO thin films pyrolyzed at 350 °C for 20 min (a) and annealed at 400 °C (b), 500 °C (c), 600 °C (d) for 2 h on glass substrates.

Figure 2 shows the XRD patterns of the CMO thin films deposited on glass substrates. It can be seen that broad and weak CMO (1 1 2) diffraction peaks appear after pyrolyzation at 350 °C for 20 min. With the increase in the annealing temperature, the diffraction intensities of CMO become stronger and sharper. Furthermore, no impurity can be observed. From these XRD results, it is clearly seen that the crystallization temperatures of the CMO thin films deposited on the Si and glass substrates using the CSD method are lower than that of bulk materials prepared by the conventional solid state reaction (about 900–1000 °C) [17], which provides a useful route to prepare CMO materials at low temperatures.

From figures 1 and 2, it is seen that the intensity ratio of (0 0 4) to (1 1 2) diffraction peaks changes with temperature. This relationship is shown in figure 3. Compared with

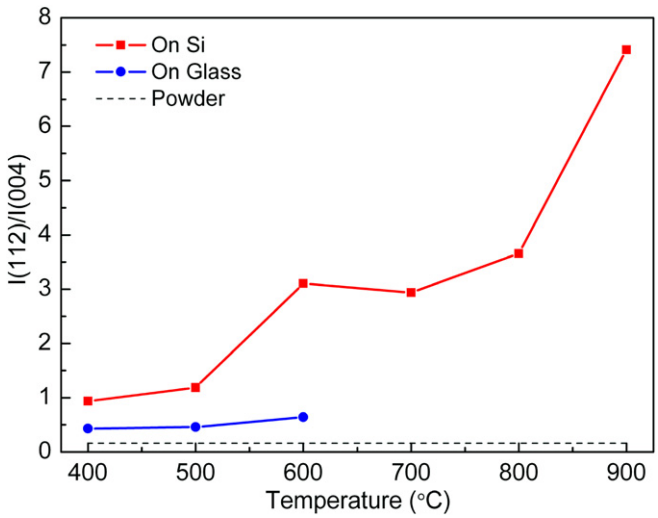

Figure 3. Intensity ratio of the (0 0 4) to (1 1 2) diffraction peak of CMO thin films on Si and glass substrates.

the intensity ratio of the powder sample, there is a *c*-axial preferential orientation for the CMO films deposited on the Si and glass substrates. The reason may be that when the CMO films are deposited on the substrate, the heterogeneous nucleation rate of crystal grains with *c*-axial orientation is higher than that with (1 1 2) orientation and the heterogeneous nucleation rate is larger than homogeneous nucleation when the contact angle is less than 180°. This results in the ratio being improved significantly. On the other hand, the ratio is increased with the increase in the annealing temperature because crystallization at higher temperatures results in a lower driving force and the heterogeneous nucleation rate will be improved further [13]. Furthermore, the ratio on Si is larger than that on glass. Because glass is an amorphous substrate and the lattice constant of Si (space group: F*d*3*m*) is 0.543 nm, which is close to the *a*-axial lattice constant of CMO (0.522 nm, space group: I41/*a*), the interface energy of CMO on Si is lower than that of CMO on glass and it results in the heterogeneous nucleation rate improving further.

The surface morphology of the CMO thin films on Si and glass annealed at different temperatures was characterized using AFM (as shown in figure 4). It is evident that the films are homogeneous and crack-free. The detailed grain size and roughness of the different samples are listed in table 1. It can be seen that the average grain size and root-mean square (rms) roughness in the $2 \times 2\ \mu m^2$ area increase with the increase in annealing temperatures and an abrupt change occurs at 600 °C. The possible reason will be discussed in the following text. Furthermore, the grain sizes of all the films are nanoscaled. The preparation of nanocrystalline CMO films at low annealing temperatures can be attributed to highly reactive nanoscaled and homogeneous precursors. On the other hand, the shape of the grains tends to change from circular to rectangular gradually with the increase in annealing temperatures. This is consistent with the crystal symmetry of CMO materials (*I*41/*a*). CMO films on Si annealed at higher temperatures (800 and 900 °C) are blurred in microscopy and too rough to be measured by AFM.

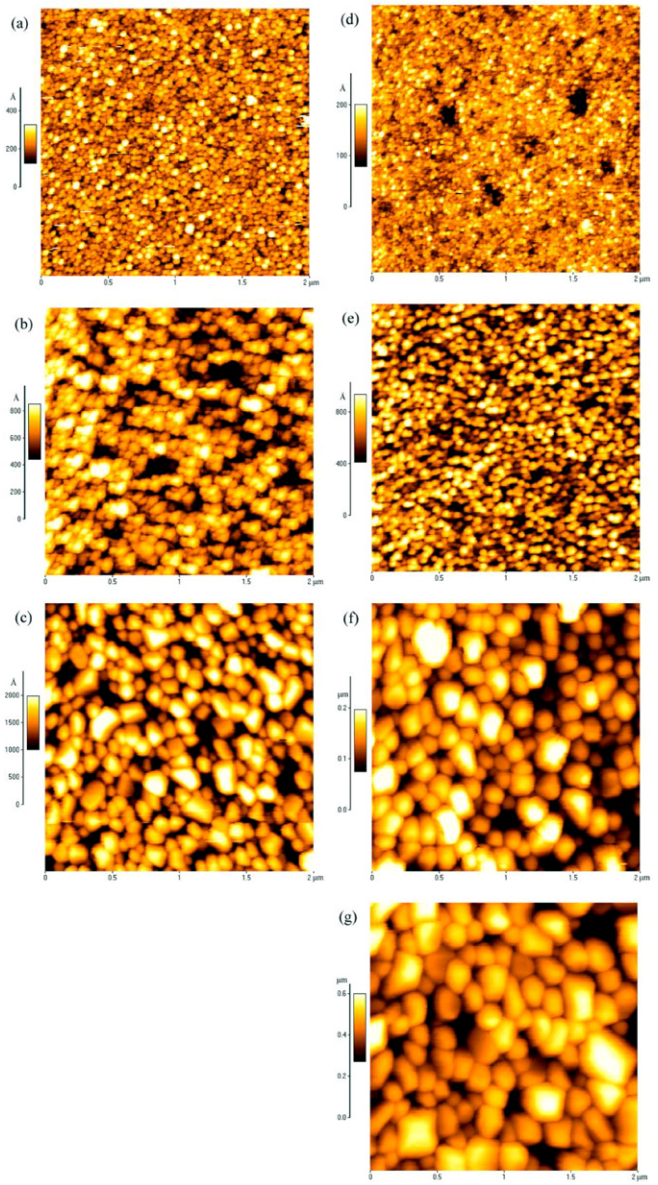

Figure 4. AFM images of CMO thin films on glass annealed at 400 °C (*a*), 500 °C (*b*), 600 °C (*c*) and on Si annealed at 400 °C (*d*), 500 °C (*e*), 600 °C (*f*), 700 °C (*g*) for 2 h respectively.

Table 1. Average grain sizes and roughnesses of CMO thin films annealed at different temperatures on Si and glass substrates.

	Glass		Si	
Temperature (°C)	Grain size (nm)	Roughness (nm)	Grain size (nm)	Roughness (nm)
400	50	4	50	2
500	75	11	60	13
600	160	28	180	34
700	—	—	264	78

An optical transmission spectrum of CMO on glass is shown in figure 5(*a*). Excellent transparency can be observed within the visible light range. The absorption edge is near 350 nm, which is consistent with the reported value of single crystal and single crystal fibre of CMO [7, 18].

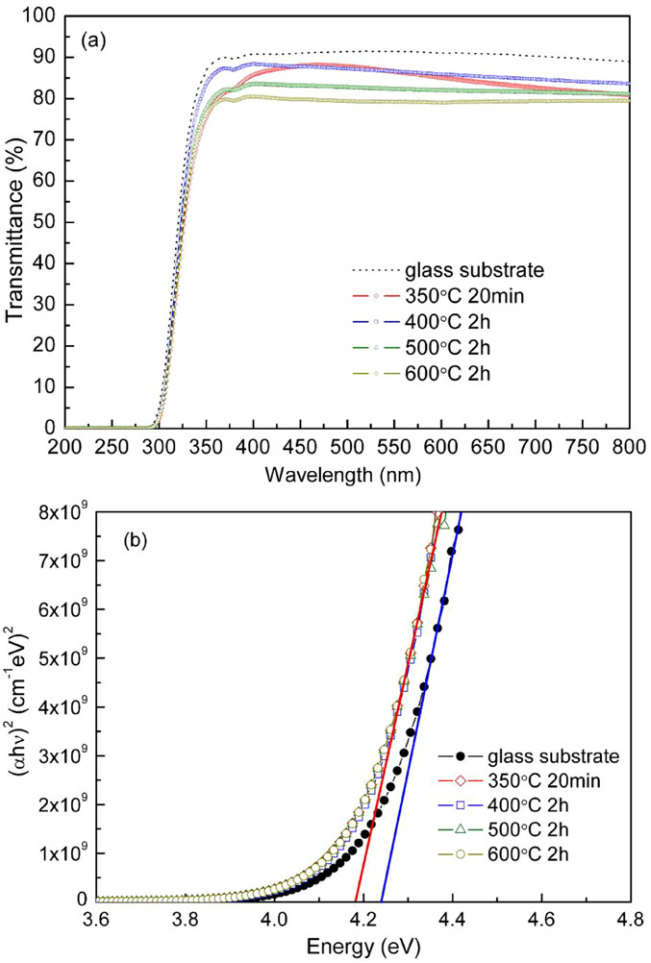

Figure 5. Transmission spectra of CMO thin films on glass annealed at different temperatures (a), the plot of $(\alpha h\nu)^2$ versus photon energy $h\nu$ and the band-gap energy is deduced from the extrapolation of the straight line up to $(\alpha h\nu)^2 = 0$ (b).

The Scheelite-type CMO has a direct band gap of 3.41 eV calculated using the linearized-augment-plane-wave method and the fundamental absorption of the CMO is attributed to a charge-transfer transition in which an oxygen 2p electron goes into one of the empty molybdenum 4d orbitals [19]. The optical energy band gap, E_{gap}, for the CMO films on glass was determined from the sharp decrease in the transmission region according to Tauc and Menth's law [20]. The plot of $(\alpha h\nu)^2$ as a function of $h\nu - E_{\text{gap}}$ is displayed in figure 5(b). The absorption coefficient, α, is influenced mainly by two factors: (i) scattering losses and (ii) fundamental absorption. At shorter wavelengths close to the optical band gap, the influence of fundamental absorption on α is more prominent than on scattering losses and α may be obtained by [21]

$$\alpha = \frac{1}{d} \ln \frac{1}{T},$$

where d is the thickness of the film and T is the transmittance of the film. In this paper, the thicknesses of the CMO films on the Si and glass substrates are about 180 and 200 nm determined using FE-SEM. In the high-energy region of the absorption edge, $(\alpha h\nu)^2$ varied linearly with $(h\nu - E_{\text{gap}})$ and

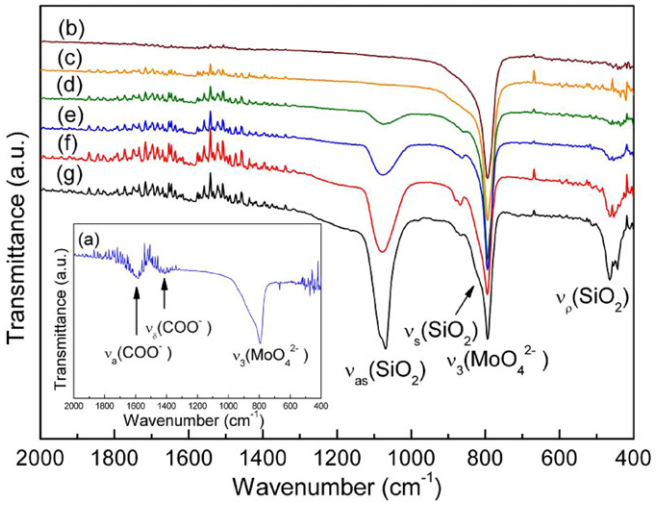

Figure 6. FT-IR transmission spectra of CMO thin films on Si pyrolyzed at 350 °C for 20 min (a) and annealed at 400 °C (b), 500 °C (c), 600 °C (d), 700 °C (e), 800 °C (f), 900 °C (g) for 2 h.

the straight line behaviour is taken as prime evidence for the direct band gap. The estimated optical band gap is 4.18 eV, which is independent of the annealing temperature, and is larger by ∼0.77 eV than the reported theoretical band-gap energy [19]. This value is acceptable because the theoretical value is underestimated [22] and a similar difference has already occurred in $CaWO_4$ [19, 23].

Figure 6 shows the FT-IR transmission spectra of CMO thin films pyrolyzed at 350 °C as well as annealed at different temperatures on Si substrates. The MoO_4^{2-} ion has tetrahedral symmetry and its representation is $\Gamma_d = A_1(\nu_1) + E(\nu_2) + F_2(\nu_3) + F_2(\nu_4)$; all modes are Raman active but $F_2(\nu_3)$ and $F_2(\nu_4)$ are IR active. The $F_2(\nu_3)$ vibrations are the antisymmetric stretches, and the $F_2(\nu_4)$ vibrations are the bending modes. From the spectrum of the CMO thin film pyrolyzed at 350 °C (figure 6(a)), undecomposed organic ligands are still present in the films. Absorption peaks at 1587 and 1413 cm^{-1} are ascribed to the stretching vibration of ν(C=O) and ν(C–O) of carboxylic groups [24]. On the other hand, there is a strong and broad absorption peak at 794 cm^{-1}. The absorption peak is assigned to $F_2(\nu_3)$ antisymmetric stretching vibration, which is suggested to originate from the Mo–O stretching vibration in the MoO_4^{2-} tetrahedron [24, 25]. It can be concluded that MoO_4^{2-} has already formed in the amorphous matrix or the CMO crystal is very small because the CMO phase has not yet been detected by XRD. Furthermore, compared with our previous results for SMO films on Si [16], it is found that the peak of $F_2(\nu_3)$ antisymmetric stretching vibrations occurring in CMO is lower than that of SMO (806 cm^{-1}). This observation is consistent with the results of other groups about the dependence of the vibrational spectra on divalent cations [26, 27].

When the films are annealed at 400–900 °C (figure 6(b)–(g)), the two peaks at 1587 and 1413 cm^{-1} disappear, meaning that the organic residua have been decomposed completely. On the other hand, broad peaks at about 1078 and 455 cm^{-1} appear at 600 °C and become stronger with the increase in the annealing temperatures; meanwhile the peak

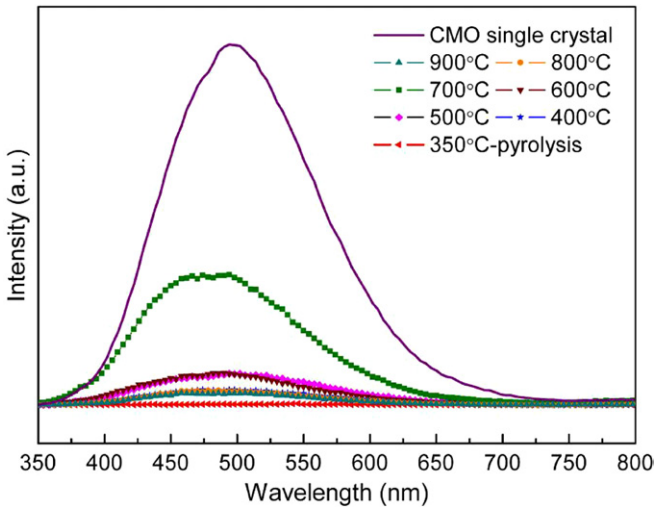

Figure 7. PL emission spectra of CMO thin films on Si pyrolyzed at 350 °C for 20 min and annealed at different temperatures for 2 h and CMO single crystal grown via the flux method.

of $F_2(\nu_3)$ vibration broadens asymmetrically and a shoulder emerges at about 815 cm^{-1}. All these peaks and shoulder can be attributed to stretching, rocking and bending vibration of SiO_2, respectively [28, 29]. That is to say, SiO_2 is generated at the interface between the Si and the CMO thin films above 600 °C, which may be the reason for the abrupt change in the grain size at this annealing temperature.

The PL spectrum of the CMO thin films on Si is shown in figure 7. With the excited wavelength at 266 nm, the CMO films exhibited a broad (∼250 nm) PL emission band in the green and blue wavelength ranges and the emission peak is located at about 490 nm, which is in accord with the previous report on CMO powders [2]. The solely green emissions are an important feature and suggest that the thin films are defect-free [30]. It is generally assumed that the measured emission spectrum of CMO is attributed mainly to the charge-transfer transitions within the MoO_4^{2-} complex [31]. Very weak PL on the pyrolyzed film at 350 °C can be attributed to no Scheelite-type format at this temperature. The intensity of PL emission in the CMO films prepared at 700 °C was stronger than those at other temperatures, implying that the PL properties of CMO films obviously depend on their morphology, sizes and crystallization. When the annealing temperature is increased, the crystallization of CMO improves and the PL intensity also becomes stronger. Above 700 °C, the surface roughness of the films abruptly increases and the films tend to be blurred. These changes influence the PL properties remarkably. On the other hand, compared with the CMO single crystal prepared by the flux method, the nanocrystalline CMO thin films had a blue-shifted emission peak by about 10 nm. This blue shift in the PL spectrum is thought to originate mainly from the quantum size effect due to the small grain size of the CMO films [32].

4. Conclusion

In summary, nanocrystalline CMO thin films of Scheelite-type have been successfully prepared on Si and soda-lime glass substrates using the CSD method at annealing temperatures from 400 to 900 °C. The crystallization of the films improves with an increase in annealing temperature. The transmission spectra of the films on glass indicate that the films are highly transparent in the visible light region and the band gap of CMO is 4.18 eV. The FT-IR spectra of annealed CMO thin films on Si presented a very intense and broad absorption band of the vibration in the MoO_4^{2-} tetrahedron. The PL emission spectra of CMO films on Si show a broad green emission band centred at 490 nm and have the strongest PL intensity for the film annealed at 700 °C, which is attributed to better crystallization quality and relatively flattened surface in microscopy. All these results indicate that CMO thin films are highly promising candidates for PL applications and the CSD method is an easy route for the preparation of CMO thin films at low temperatures on different substrates.

Acknowledgments

This work was supported by the National Key Basic Research Program of China under contract No 2006CB601005, the National Natural Science Foundation of China under contract No 10774146, the Anhui Province NSF Grant No 070414162, the Director's Fund of Hefei Institutes of Physical Science and the Fund of Chinese Academy of Sciences for Excellent Graduates.

References

[1] Sleight W 1972 *Acta Crystallogr.* B **28** 2899
[2] Yoon J-W, Ryu J H and Shim K B 2006 *Mater. Sci. Eng.* B **127** 154
[3] Ivleva L I, Basiev T T, Voronina I S, Zverev P G, Osiko V V and Polozkov N M 2003 *Opt. Mater.* **23** 439
[4] Mikhailik V B, Kraus H, Wahl D and Mikhailik M S 2005 *Phys. Status Solidi* B **242** R17
[5] Graser R, Pitt E, Scharmann A and Zimmerer G 1975 *Phys. Status Solidi* B **69** 359
[6] Johnson L F, Boyd G D, Nassau K and Soden R R 1962 *Phys. Rev.* **126** 1406
[7] Korzhik M V *et al* 2008 *IEEE Trans. Nucl. Sci.* **55** 1473
[8] Choi G K, Cho S Y, An J S and Hong K S 2006 *J. Eur. Ceram. Soc.* **26** 2011
[9] Lei F and Yan B 2008 *J. Solid State Chem.* **181** 855
[10] Yu P, Bi J, Xiao D Q, Chen L P, Jin X L and Yang Z N 2006 *J. Electroceram.* **16** 473
[11] Chen L and Gao Y 2007 *Chem. Eng. J.* **131** 181
[12] Cho W S, Yashima M, Kakihana M, Kudo A, Sakata T and Yoshimura M 1997 *J. Am. Ceram. Soc.* **80** 765
[13] Schwartz R W 1997 *Chem. Mater.* **9** 2325
[14] Lei H C, Sun Y P, Zhu X B, Song W H, Yang J and Gu H W 2007 *IEEE Trans. Appl. Supercond.* **17** 3819
[15] Singh S K, Ishiwara H and Maruyama K 2006 *Appl. Phys. Lett.* **88** 262908
[16] Lei H C, Zhu X B, Sun Y P and Song W H 2008 *J. Cryst. Growth* **310** 789
[17] Hitoki G, Takata T, Ikeda S, Hara M, Kondo J N, Kakihana M and Domen K 2000 *Catal. Today* **63** 175
[18] Barbosa L B, Ardila D R, Cusatis C and Andreeta J P 2002 *J. Cryst. Growth* **235** 327
[19] Zhang Y, Holzwarth N A W and Williams R T 1998 *Phys. Rev.* B **57** 12738

[20] Tauc J and Menth A 1972 *J. Non-Cryst. Solids* **8–9** 569
[21] Aarik J, Aidla A, Kiisller A A, Uustare T and Sammelselg V 1997 *Thin Solid Films* **305** 270
[22] Marques A P A, de Melo D M A, Longo E, Paskocimas C A, Pizani P S and Leite E R 2005 *J. Solid State Chem.* **178** 2346
[23] Maurera M A M A, Souza A G, Soledade L E B, Pontes F M, Longo E, Leite E R and Varela J A 2004 *Mater. Lett.* **58** 727
[24] Nakamoto K 1986 *Infrared and Raman Spectra of Inorganic and Coordination Compounds* 4th edn (New York: Wiley)
[25] Marques A P A, Melo D M A, Paskocimas C A, Pizani P S, Joyac M R, Leite E R and Longo E 2006 *J. Solid State Chem.* **179** 671
[26] Marques A P A, Leite E R, Varela J A and Longo E 2008 *Nanoscale Res. Lett.* **3** 152
[27] Basiev T T, Sobol A A, Voronko Y K and Zverev P G 2000 *Opt. Mater.* **15** 205
[28] Tsu D V, Lucovsky G and Davidson B N 1989 *Phys. Rev.* B **40** 1795
[29] Lucovsky G, Manitini M J, Srivastava J K and Irene E A 1987 *J. Vac. Sci. Technol.* B **5** 530
[30] Yoshimura M, Ohmura M, Cho W S, Yashima M and Kakihana M 1997 *J. Am. Ceram. Soc.* **80** 2464
[31] Mikhrin S B, Mishin A N, Potapov A S, Rodnyi P A and Voloshinovskii A S 2002 *Nucl. Instrum. Methods* A **486** 295
[32] Lu S G, Mak C L, Pang G K H, Wong K H and Cheah K W 2008 *Nanotechnology* **19** 035702